International Journal of Speleology	46 (3)	345-358	Tampa, FL (USA)	September 2017

Available online at scholarcommons.usf.edu/ijs

International Journal of Speleology

Official Journal of Union Internationale de Spéléologie

The impact of door opening on CO_2 levels: A case study from the Balcarka Cave (Moravian Karst, Czech Republic)

Marek Lang[1*], Jiří Faimon[1,2], and Sandra Kejíková[1]

[1]Department of Geological Sciences, Faculty of Sciences, Masaryk University, Kotlářská 2, 611 37 Brno, Czech Republic
[2]Department of Geology, Faculty of Science, Palacký University Olomouc, 17. listopadu 1192/12, 771 46 Olomouc, Czech Republic

Abstract: The impact of door opening on cave carbon dioxide (CO_2) levels was studied in the Entrance Chamber and the Gallery Chamber of the Balcarka Cave (Moravian Karst, Czech Republic). The effect of door opening differed with cave ventilation modes. Under upward airflow mode, the cave door opening led to the increase of output advective CO_2 fluxes from the cave and to the decrease of CO_2 levels. This effect was evident especially in the Entrance Chamber near the cave entrance and then suppressed in the Gallery Chamber situated deeper in the cave. Under the downward airflow mode, the cave door opening changed airflow paths and main CO_2 sources/fluxes. This resulted in the increase of CO_2 level in the Entrance Chamber while the levels in the Gallery Chamber decrease. Modeling indicates that the increase could be result of input advective CO_2 fluxes from epikarst (up to 5.9×10^{-2} mol s^{-1}). To reduce the impact on cave microclimate, a careful control of the visiting regime without overlapping of individual doors' openings is recommended.

Keywords: cave chamber, CO_2 levels, cave ventilation, door opening, advective CO_2 flux

Received 6 December 2016; Revised 29 April 2017; Accepted 29 April 2017

Citation: Lang M., Faimon J. and Kejíková S., 2017. The impact of door opening on CO_2 levels: A case study from the Balcarka Cave (Moravian Karst, Czech Republic). International Journal of Speleology, 46 (3), 345-358. Tampa, FL (USA) ISSN 0392-6672
https://doi.org/10.5038/1827-806X.46.3.2100

LIST OF SYMBOLS

A	total diffusion area [m^2]
c_{CO2}	carbon dioxide concentration [mol m^{-3}]
c_{EK}	carbon dioxide concentration in soils/epikarst [mol m^{-3}]
c_{Gal}	carbon dioxide concentration in Gallery Chamber [mol m^{-3}]
Δc	difference in carbon dioxide concentrations [mol m^{-3}]
D	carbon dioxide diffusion coefficient [m^2 s^{-1}]
j	total carbon dioxide flux [mol s^{-1}]
j_{adv}	input advective carbon dioxide flux [mol s^{-1}]
j_{deg}	input carbon dioxide flux derived from one liter of dripwater by degassing [mol s^{-1}]
j_{dif}^{EK}	total input diffusive carbon dioxide flux from soils/epikarst [mol s^{-1}]
j_{adv}^{EK}	input advective carbon dioxide flux from soils/epikarst [mol s^{-1}]
j_{adv}^{Gal}	input advective carbon dioxide flux from Gallery Chamber [mol s^{-1}]
ΔL	overburden thickness [m]
P	barometric pressure [Pa]
Q	volumetric airflow rate [m^3 s^{-1}]
R	the universal gas constant [J kg^{-1} K^{-1}]
P_{CO2}	carbon dioxide partial pressure [dimensionless]
$^{(C)}P_{CO2}$	carbon dioxide partial pressure in cave atmosphere [dimensionless]
$^{(H)}P_{CO2}$	hypothetical P_{CO2} reconstructed from cave dripwater chemistry [dimensionless]
$^{(W)}P_{CO2}$	carbon dioxide partial pressure in water [dimensionless]
t	time [s]
T	temperature [°C]
T_{cave}	temperature in cave atmosphere [°C]
$T_{exterior}$	temperature in external atmosphere [°C]
ΔT	temperature difference [°C]
v	linear airflow rate [m s^{-1}]
V	cave total volume [m^3]

ABBREVIATIONS

C1-UAF	campaign 1; upward airflow
C2-DAF	campaign 2; downward airflow
C3-DAF	campaign 3; downward airflow
C4-DAF	campaign 4; downward airflow
CC	Chimney Chamber
CD	connecting door
CO_2	carbon dioxide
DAF mode	downward airflow ventilation mode

*mareklang@mail.muni.cz

DMC-DAF	detailed monitoring campaign; downward airflow
EC	Entrance Chamber
GC	Gallery Chamber
UAF mode	upward airflow ventilation mode

INTRODUCTION

Carbon dioxide (CO_2) is an important component of the global carbon cycle (e.g., Schlesinger & Andrews, 2000) and plays important role in many karst processes such as limestone dissolution (e.g., Stumm & Morgan, 1996), calcite speleothem formation (e.g., Dreybrodt, 1999; Banner et al., 2007; Frisia et al., 2011), or speleothem corrosion (e.g., Sarbu & Lascu, 1997; Dublyandsky & Dublyansky, 1998; Tarhule-Lips & Ford, 1998; Faimon et al., 2006). The difference between the CO_2 partial pressures in (1) soil/upper epikarst, $^{(H)}P_{CO2}$, and (2) cave atmosphere, $^{(C)}P_{CO2}$, represents the driving force for these processes (White, 1988; Ford & Williams, 2007). Some studies showed that hypothetical $^{(H)}P_{CO2}$ values could be reconstructed from cave dripwater hydrogeochemistry (Faimon et al., 2012c; Peyraube et al., 2013; Milanolo & Gabrovšek, 2015; Pracný et al., 2016a, b). Generally, enhanced $^{(H)}P_{CO2}$ (Fairchild et al., 2000; Faimon et al., 2012c) is responsible for limestone dissolution and cave development (Baldini et al., 2006). The lower $^{(C)}P_{CO2}$ controls dripwater degassing and calcite precipitation (speleothem growth) (Holland et al., 1964).

It is well known that the environment of show caves is significantly influenced by (1) human activity derived from the works required for ensuring the access of cave visitors, and by (2) presence of visitors inside the cave. The anthropogenic impact in show caves was documented by many studies focused on (i) temperature (e.g., Pulido-Bosch et al., 1997; de Freitas & Schmekal, 2006; Šebela & Turk, 2014), (ii) CO_2 concentrations (Faimon et al., 2006; Liñán et al., 2008; Milanolo & Gabrovšek, 2009; Šebela et al., 2013; Lang et al., 2015a), and (iii) both the components above (e.g., Hoyos et al., 1998; Sánchez-Moral et al., 1999; de Freitas, 2010). In addition, there were some attempts to summarize the principles of optimum cave management and cave environment conservation (e.g., Fernández et al., 1986; Calaforra et al., 2003; Lario & Soler, 2010; Lobo, 2015; Lang et al., 2017). In addition to former "standard" phenomena, so-called "parasitic phenomena" may also be recognized in caves. This term was adopted from electrical engineering. It represents various adverse phenomena that distort time series of basic variables. In cave environment, such phenomena could be associated especially with temporary anthropogenic interventions into the cave microclimate. As an example, Lang et al. (2015b) recently presented the study of the visitor movement in low-profile passages that affect cave ventilation and disturb or even make inverse the CO_2 level evolution. Another similar phenomenon is linked to door opening. The caves made available to tourists are often equipped with doors to protect cave microclimate. However, the high attendance in show caves is associated with the frequent cave door opening during visiting hours, which could contribute to changes in the cave ventilation and consequently in CO_2 levels. The goal of this work was to verify in detail the impact of cave door opening on (i) cave ventilation and (ii) cave CO_2 levels based on a case study in the Balcarka Cave (Moravian Karst).

METHODS

Site of study

The Balcarka Cave is situated in the northern part of the Moravian Karst near the Ostrov u Macochy village (Faimon et al., 2012a; Lang et al., 2015a, b). The position and sketch map of the cave are illustrated in Fig. 1A. Mean annual precipitation in the study area is about 700 mm; mean annual temperature of the external atmosphere is about 10°C (Pracný et al., 2016a). The cave has been formed in the Upper Devonian limestones of the Macocha Formation. It consists of a two-level complex of relatively narrow corridors (total length of about 350 m) and the chambers. The cave is known for rich speleothem decoration of all types: stalactites/stalagmites, flowstones, curtains, and thick-walled soda straws. The height distance between both cave levels is about 20 m. The thickness of cave rock overburden is about 20-50 m (Fig. 1B). The cave has three entrances equipped by steel doors: the main entrance #1 is at 459.3 m above sea level (a.s.l.), the old cave exit #3 at 457.5 m a.s.l., and the new cave exit #4 at 446.9 m a.s.l. (Fig. 1B). Additional doors, the door #2 and the connecting door (CD) separate the input cave portal from the Entrance Chamber and the Chimney Chamber, respectively (Fig. 1). Note that only doors #1 (entrance into the cave), #2 (input to the Entrance Chamber) and #4 (exit from the cave) are used during visitor tours, doors #3 and CD were opened only for the purpose of the experimental monitoring. In addition to the known entrances, some hidden/unknown openings undoubtedly exist in the cave. All the entrances/openings in distinct altitudes are responsible for the dynamic behavior of cave air circulation. A theoretical background on cave air circulation was given by Cigna (1968) and Wigley & Brown (1971). Several studies on artificial systems (e.g., Richon et al., 2005) can also be useful for the better understanding natural systems. The cave airflows principally depend on (1) cave geometry and (2) the pressure difference resulting from contrasting air densities (de Freitas et al., 1982; Kowalczk & Froelich, 2010). Since density is primarily a function of temperature, cave airflows are mostly related to the temperature difference between external and cave atmospheres, $\Delta T = T_{exterior} - T_{cave}$ (where $T_{exterior}$ is external air temperature and T_{cave} is cave air temperature [°C]) (Baker & Genty, 1998; Bourges et al., 2001; Spötl et al., 2005; Faimon et al., 2012a; Faimon & Lang, 2013). Based on sign of the temperature difference, two ventilation regimes are distinguished. When $\Delta T < 0$, upward airflows occur and cave is in the *upward airflow ventilation mode* (*UAF* mode). If $\Delta T > 0$, the cave airflow direction is opposite; this corresponds to the *downward airflow ventilation mode* (*DAF* mode) (see Faimon et

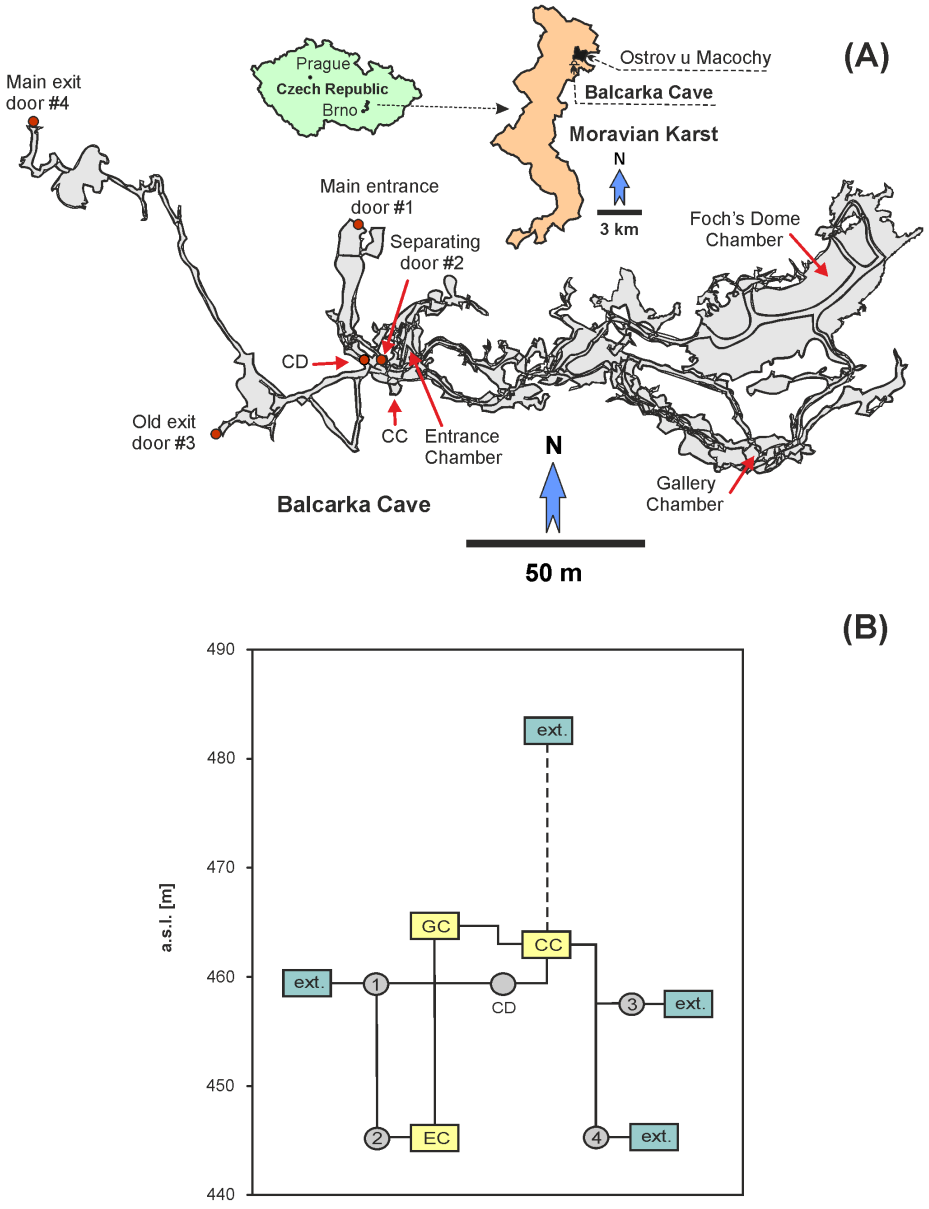

Fig. 1. The Balcarka Cave location and the cave sketch map with monitoring sites (A). The altitude diagram of the individual cave passages (B). The acronyms correspond to Entrance Chamber (EC), Gallery Chamber (GC), Chimney Chamber (CC), and exterior (ext.).

al., 2012a for details). Based on Lang et al. (2015b), the hypothetical natural airflow into the Balcarka Cave reaches up to 3.2 × 10^{-3} m^3 s^{-1}. Based on case measurements in the cave, the natural CO_2 levels are well known for winter seasons when the cave is out of visiting regime. They approach the external CO_2 levels about 400-500 ppmv. In summer seasons, the peak CO_2 values can reach up to 7,000 ppmv (see Faimon et al., 2012c). However, these values are affected by the visitors' breathing (see Lang et al., 2015a, b). The annual course of the cave CO_2 clearly indicates a dynamic cave of type B (Lang et al., 2016). Since 1923, the Balcarka cave was gradually explored from different sites; the individual cave parts were merged together in 1936. The cave became public in 1926; the visitor circuit was modified into the current state in 1949. Nowadays, the cave is open to tourists from March to November; the attendance is about 30,000 to 40,000 persons per year. The daily visiting regime covers several tours: average three tours per day during early spring (late fall) are expanding to average ten tours per day during summer. Whereas the entries of individual groups start every hour in case of the smaller number of groups, the intervals between groups are shortened to half an hour in case of higher number of groups. The visit duration is about one hour. It indicates that up to three visitor groups may be simultaneously present in the cave (while one group is entering the cave, second group is inside, and third group is leaving the cave).

The Entrance Chamber (EC) and the Gallery Chamber (GC) were chosen as the monitoring sites (Fig. 1). The EC with total volume of about ~110 m^3 is situated in the lower cave level, approximately 50 m from the cave entrance. The chamber is developed in the low-profile cave passages with the cross section from 3 to 7 m^2. The chamber input passage is represented by a narrow corridor with descending staircase. In contrast, the output passage from the chamber is represented by the narrow corridor of about ~60 m long leading into the large Foch's Dome Chamber. The GC with total volume of about ~150 m^3 is developed in deeper cave passages. It roughly corresponds to homothermic zone (see Luetscher &

Jeannin, 2004 for details). The chamber is situated in the upper cave level and it is accessible by ascending/descending staircases.

Monitoring

Time series of CO_2 concentrations were collected during five individual monitoring campaigns designed on the basis of the external temperature (in the period from November 2013 to July 2015). Because Balcarka Cave represents a show cave, all the campaigns were conducted in the late afternoon, when the cave was closed to visitors. Individual measuring sensors were placed into the chambers after the last visitor group had left the cave, about ~1 hour before start of experiment. Based on some studies on anthropogenic CO_2 dynamics (e.g., Lang et al., 2017), the period of 1 hour without anthropogenic influence leads to the significant decrease of anthropogenic CO_2 in the cave atmosphere. Further decrease has slower dynamics than the changes induced by door opening. The individual campaigns were divided into fifteen ten-minute intervals. Each interval was connected with opening of different cave door combinations. The ten-minute intervals at individual combination were assumed to be sufficiently long to identify the changes induced by door opening and sufficiently short for excluding some others influences (e.g., the changes in barometric pressure, external temperature, and other variables). A monitoring schedule of door opening during the individual campaigns is given in Table 1. The order of door combinations was designed to keep the continuity of airflow changes. The temperatures for ΔT calculations were logged with 1-minute time steps (i) in the exterior, about 50 m outside the cave, and (ii) inside the cave in the Entrance Chamber, about 50 m from the main entrance (door #1). Based on the previous monitoring in the Balcarka Cave, the temperature difference between EC and GC do not exceed 1°C, therefore the temperature in both chambers was assumed consistent. During the campaign DMC-DAF, airflow was logged at 10-second time steps at one point in slightly open separating door (#2) (the surface area of the gap corresponded to 0.1 m^2). The schedule of all the campaigns is in Table 2.

Table 1. Monitoring schedule of door opening (Balcarka Cave, Moravian Karst).

Campaigns C1-UAF and C2-DAF		Campaigns C3-DAF and C4-DAF	
Elapsed time [min]	**Door combination**	**Elapsed time [min]**	**Door combination**
0 - 10	#1	0 - 10	#1
11 - 20	#1 + #2	11 - 20	#1 + #2
21 - 30	#2	21 - 30	#2
31 - 40	#1 + #2 + #3	31 - 45 (36 - 40)	#1 + #2 + #3 (#1 + #2 + #3 + CD)
41 - 50	#1 + #2 + #3 + #4	46 - 55	#1 + #2 + #3 + #4
51 - 60	#1 + #2 + #4	56 - 65	#1 + #2 + #4
61 - 70	#2 + #4	66 - 75	#2 + #4
71 - 80	#2 + #3 + #4	76 - 85	#2 + #3 + #4
81 - 90	#2 + #3	86 - 100 (91 - 95)	#2 + #3 (#2 + #3 + CD)
91 - 100	#3	101 - 110	#3
101 - 110	#3 + #4	111 - 120	#3 + #4
111 - 120	#1 + #3	121 - 130	#1 + #3
121 - 130	#1 + #3 + #4	131 - 140	#1 + #3 + #4
131 - 140	#1 + #4	141 - 150	#1 + #4
141 - 150	#4	151 - 160	#4

Table 2. Schedule of monitoring campaigns.

Campaign	Ventilation mode	Date	T_{ext} [°C]	T_{cave} [°C]	ΔT [°C]	Monitored variables	Measurement period [min]
C1-UAF	UAF	2-Dec-13	6.8 to 7.4	8.7	-1.8 to -1.2	CO_2, $T_{exterior}$, T_{cave}	150
C2-DAF	DAF	3-Jul-15	28.1 to 30. 6	9.0 to 9. 6	19.0 to 21.2	CO_2, $T_{exterior}$, T_{cave}	150
C3-DAF	DAF	29-Apr-16	13.8 to 17.6	8.3 to 10.0	5.2 to 7.7	CO_2, $T_{exterior}$, T_{cave}	160
C4-DAF	DAF	30-Jul-16	23.4 to 27.2	9.4 to 11.1	13.9 to 17.7	CO_2, $T_{exterior}$, T_{cave}	160
DMC-DAF	DAF	27-Aug-16	26.0 to 29.6	n.m.	n.m.	CO_2, $T_{exterior}$, airflows	90

n.m. - not measured

The CO_2 concentrations were measured with 1-minute time steps in EC and GC at about 2 m above the cave floor. During all the campaigns, CO_2 concentrations were monitored under conditions without the visitor presence inside the cave (without anthropogenic influence). The CO_2 was detected by a 2-channel IR-detector FT A600-CO2H (measuring range: 0 to 10,000 ppmv; accuracy: ±50 ppmv + 2 vol. % of measured value in the range of 0 to 5,000 ppmv; resolution: 1 ppmv or 0.0001 vol. %) linked to the ALMEMO 2290-4 V5 Ahlborn data logger (Germany). For modeling, the volume concentrations (in ppmv unit) were consecutively recalculated into molar concentrations (mol m^{-3}), based on the Ideal Gas Law and given temperature/pressure,

$$c_{CO2}\ [\text{mol m}^{-3}] = \frac{P}{10^6\ RT} c_{CO2}\ [\text{ppmv}] \qquad (1)$$

where P is barometric pressure [Pa], R is the universal gas constant [R = 8.3144621 J kg^{-1} K^{-1}] and T is temperature [K]. Data on barometric pressure were obtained from the meteorological station Vranov at similar altitude of 484 m a.s.l. for the campaigns C4-DAF and DMC-DAF. As the data for the remaining campaigns (C1-UAF, C2-DAF, C3-DAF) were unavailable at this station, the pressure data were compiled and recalculated from alternative stations: Brno - Kraví Hora (280 m a.s.l.), Otinoves (565 m a.s.l.), and Vysočany (580 m a.s.l.). The final data range from 103,000 to 103,250 Pa (C1-UAF), from 102,662 to 102,700 Pa (C2-DAF), and from 101,578 to 102,024 Pa (C3-DAF). For C4-DAF and DMC-DAF, respectively, the mean values of 101,522 and 102,190 Pa were used. The applying these values for c_{CO2} calculation (Eq. 1) showed only slight deviations from calculations with standard barometric pressure of 101,325 Pa.

The temperatures for ΔT calculations were logged (i) in the exterior, approximately 50 m from the cave entrance, and (ii) in EC. It was measured by COMET S3120 data loggers (measuring range from -30 to +70°C with a precision of ±0.4°C). Airflows were measured by the FVA935 TH4 thermo-anemometer-sensor (measuring range from 0.05 to 2 m s^{-1} with a precision of ±0.04 m s^{-1}) connected with the ALMEMO 2290-4 V5 data logger (Ahlborn, Germany). The linear airflow rate, v [m s^{-1}], was consecutively recalculated into volumetric airflow rate, Q [m^3 s^{-1}], based on the section area through which air flowed.

THEORETICAL BACKGROUND

The concentration of CO_2 in cave atmosphere is result of balancing of various input and output CO_2 fluxes. The principal fluxes are: (i) diffusive CO_2 fluxes, (ii) advective CO_2 fluxes, and (iii) CO_2 flux derived from dripwater degassing.

The total input diffusive CO_2 flux from soils/epikarst, j_{dif}^{EK} [mol s^{-1}], is believed to represent the principal input CO_2 flux into cave chamber. It can be estimated based on the Fick's First Law:

$$J_{dif}^{EK} = -D\ A \frac{\Delta c}{\Delta L} \qquad (2)$$

where D is CO_2 diffusivity (diffusion coefficient) in karst bedrock [m^2 s^{-1}], A is the total area through which CO_2 diffuses into the cave chamber [m^2], and Δc/ΔL is the concentration gradient given by the concentration difference Δc [mol m^{-3}] over the distance ΔL [m]. The CO_2 diffusivity is rather uncertain due to karst profile/bedrock inhomogeneity (limestone, soils/sediments, fissures, cracks, or shafts). It varies in the wide range from 1.0 × 10^{-7} m^2 s^{-1} (Davidson & Trumbore, 1995) to 1.4 × 10^{-5} m^2 s^{-1} (Welty et al., 2008). The concentration difference, Δc, was assumed to be the difference between CO_2 concentrations in soil/epikarst and cave atmosphere.

The advective CO_2 fluxes across the cave, j_{adv} [mol s^{-1}], are given by the equation

$$j_{adv} = Q\ c_{CO2} \qquad (3)$$

where Q is the volumetric airflow rate [m^3 s^{-1}] and c_{CO2} is CO_2 concentration [mol m^{-3}]. The positive advective fluxes correspond to the airflow direction into cave and negative ones to the airflow direction out of cave. The flux sign is derived from the sign of airflow volumetric velocity. The effects of the advective CO_2 fluxes may differ, depending on airflow direction and position inside cave. Whereas the airflow from exterior decreases the CO_2 level, the airflow transporting CO_2 from deeper cave sites and epikarst can increase the level (Lang et al., 2015a).

The input CO_2 flux derived from dripwater degassing, j_{deg} [mol s^{-1}], is generally a significant contributor to CO_2 in a cave chamber. The infiltrating water saturated by gaseous CO_2 (at given P_{CO2} in soils/epikarst) typically degasses after reaching the cave (Holland et al., 1964; Bourges et al., 2001; Baldini et al., 2008). The degassing driving force is the difference between (1) partial pressure of CO_2 in the water, ${}^{(W)}P_{CO2}$, (i.e., partial pressure of gaseous CO_2 at equilibrium with aqueous carbonate species) and (2) actual partial pressure of CO_2 in cave atmosphere, ${}^{(C)}P_{CO2}$ (Faimon et al., 2006; Ford & Williams, 2007; Faimon et al., 2012a). In this work, however, such flux was considered constant because of the short duration of the experiments. Thus, the effect of the flux at door opening was ignored.

The total CO_2 flux into a cave chamber, j [mol s^{-1}], is given as the sum of the all CO_2 fluxes (input fluxes are positive, output ones are negative),

$$j = \sum_i j_i \qquad (4)$$

where j_i are the individual fluxes [mol s^{-1}]. Several studies based on dynamics modeling and mass fluxes (e.g., Holland et al., 1964; Lasaga & Berner, 1998; Richon et al., 2005) are inspiring. Alternatively, the total CO_2 flux may be obtained from the slope of CO_2 time series based on the relation

$$j = \frac{Vdc}{dt} \qquad (5)$$

where V is cave chamber volume [m^3], c is instantaneous CO_2 concentration in the chamber atmosphere [mol m^{-3}], and t is time [s].

DATA

Monitoring during UAF ventilation mode (C1-UAF period)

The raw data (2.5-hour-long time series) obtained during the monitored campaign C1-UAF (5 November 2013) comprise the CO_2 concentrations from EC/GC and the temperature difference $\Delta T = T_{ext} - T_{cave}$ (Fig. 2). All the data were collected during the period of active ventilation at the external temperature between 6.8 and 7.4°C. Based on almost constant cave site temperature (T_{cave} ~8.7°C), the temperature difference ΔT ranged from -1.8 to -1.2°C (Fig. 2A). It indicates that cave persisted in the upward airflow (UAF)

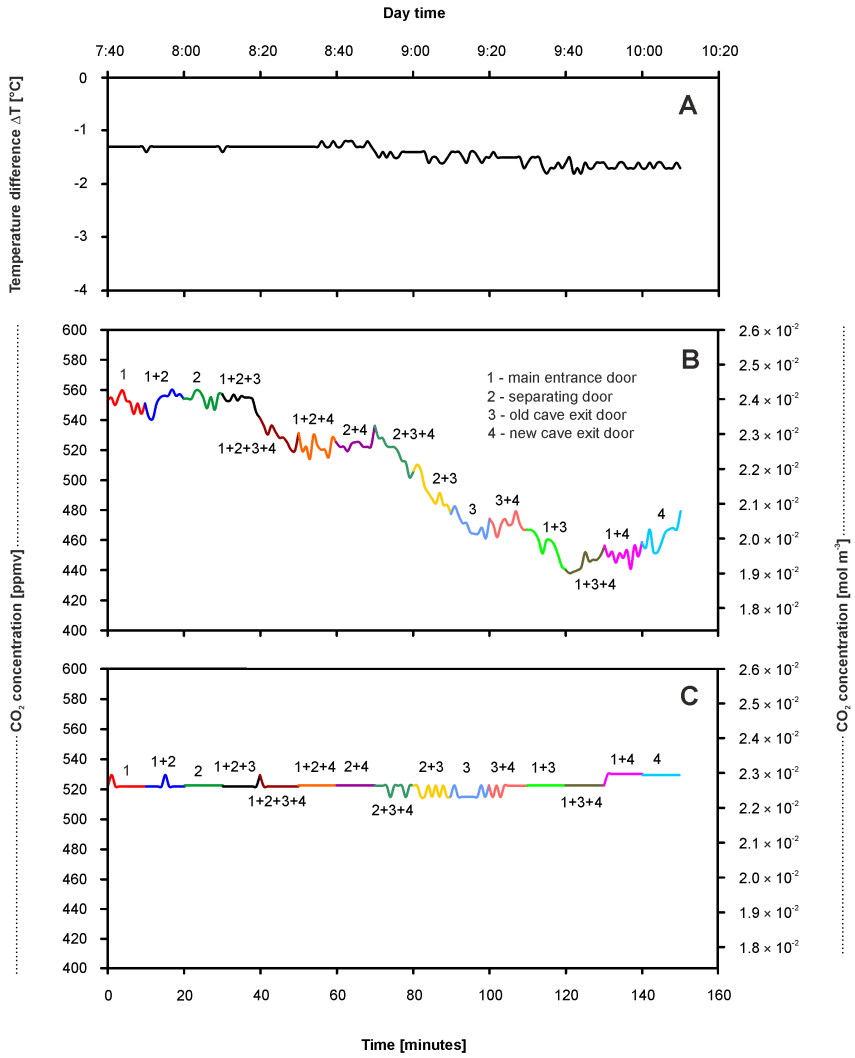

Fig. 2. Data from the campaign C1-UAF (5 November 2013; Balcarka Cave): temperature difference ΔT (A) and CO_2 concentrations in Entrance Chamber (B) and Gallery Chamber (C). The numbers at curves represent numbers of the doors open for given period. See text for details.

ventilation mode during the whole campaign. These data show different evolution in individual chambers. Whereas CO_2 concentrations gradually decrease from 560 to 438 ppmv (2.4×10^{-2} to 1.9×10^{-2} mol m^{-3}) in EC during various combinations of door opening (Fig. 2B), almost constant values with fluctuation of about 15 ppmv (6.5×10^{-4} mol m^{-3}) were observed in GC (Fig. 2C).

Monitoring during DAF ventilation mode

During the DAF mode, four monitoring campaigns were performed (Table 1). At the first campaign C2-DAF, a surprising behavior of CO_2 was observed. The next two campaigns, C3-DAF and C4-DAF, aimed to verify the data from the previous campaign. The last campaign DMC-DAF was focused on detail CO_2 monitoring and airflow direction/rates.

Campaign C2-DAF

During this 2.5-hour-long campaign (running in 3 July 2015), external temperature ranged from 28.1 to 30.6°C. The cave persisted in the period of active ventilation. Based on almost constant cave site temperature (T_{cave} ~9.0 to 9.6°C), the temperature difference ΔT ranged from 19.0 to 21.2°C (Fig. 3A). This indicates the downward airflow (DAF) ventilation mode during the whole campaign. The CO_2 concentrations in EC varied in the wide range from 464 to 1,187 ppmv (2.0×10^{-2} to 5.1×10^{-2} mol m^{-3}) (Fig. 3B). Based on the evolution of CO_2 concentrations in EC, two main groups of door combinations were identified. Whereas some combinations (open door #1+#2+#3, or #2+#3) led to the increase of CO_2 levels, other combinations (open door #1+#2+#4, #1+#4) resulted in the decrease of CO_2 levels. In contrast to EC, the concentrations in GC systematically decreased from 1,430 ppmv to 1,176 ppmv (6.2×10^{-2} to 5.1×10^{-2} mol m^{-3}) (Fig. 3C).

Campaign C3-DAF

During this 2.7-hour-long campaign (running in 29 April 2016), the schedule of door opening was expanded by the two 5-minute intervals with the open connecting door CD (Fig. 1). The campaign was implemented into monitoring schedule based on the experience from the campaign C2-DAF, when the door was opened accidentally. The 5-minute periods of the CD opening were chosen in order to distinguish clearly the role of CD in ventilation regime. Based on the external temperature ($T_{exterior}$ ~13.8 to 17.6°C) and cave site temperature (T_{cave} ~8.3 to 10.0°C), the temperature difference ΔT ranged from 5.2 to 7.7°C (Fig. 4A). It indicates that cave persisted in downward

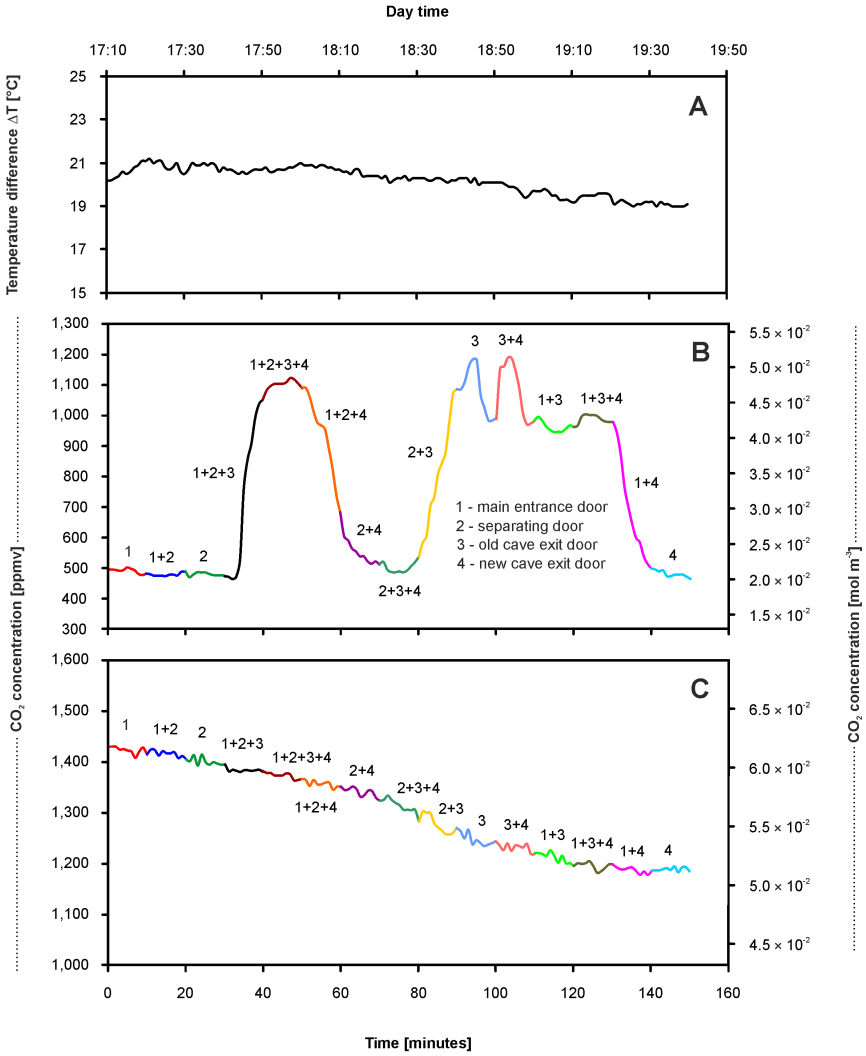

Fig. 3. Data from the campaign C2-DAF (3 July 2015; Balcarka Cave): temperature difference ΔT (A) and CO_2 concentrations in Entrance Chamber (B) and Gallery Chamber (C). The numbers at curves represent numbers of the doors open for given period. See text for details.

airflow (DAF) ventilation mode during the whole campaign. The CO_2 concentrations in EC varied around mean value of ~480 ppmv (2.1×10^{-2} mol m^{-3}) (Fig. 4B). Despite the relatively narrow range, two different trends were identified in CO_2 level evolution depending on the door opening combinations. In the case of periods with the open doors #1+#2+#3+#4 or #3, slight increase of CO_2 levels is observed. However, systematical decrease of CO_2 levels is evident during the periods with the open doors #2+#4 and #1+#3+#4. In GC, the "natural" CO_2 levels (without anthropogenic influence) varied around mean value of ~500 ppmv (2.2×10^{-2} mol m^{-3}) (Fig. 4C).

Campaign C4-DAF

This 2.7-hour-long campaign (running in 30 July 2016) followed the campaign C3-DAF. It includes two 5-minute intervals with open connecting door CD. The external temperature ranging from 23.4 to 27.2°C indicates that cave persisted in the period of active ventilation. Based on the cave site temperature (T_{cave} ~9.4 to 11.1°C), the temperature difference ΔT ranged from 13.9 to 17.7°C (Fig. 5A), which indicates DAF ventilation mode during the whole campaign. The CO_2 concentrations in EC varied in a wide range between 352 and 2,058 ppmv (1.5×10^{-2} and 8.9×10^{-2} mol m^{-3}) (Fig. 5B). The lower-than-mean CO_2 concentrations in the external atmosphere are in the range of the diurnal variations of 371 ± 65 (STDEV) ppmv monitored in a local meteorological station Holštejn. Whereas some combinations of door opening (#1+#2+#3 and #2+#3) correspond to the rapid increase of the CO_2 levels, other combinations (#1+#2+#3+#4 and #1+#2+#4) represent quick decrease of CO_2 levels. In GC, the concentrations systematically decrease from 3,413 to 2,697 ppmv (1.5×10^{-1} to 1.2×10^{-1} mol m^{-3}) (Fig. 5C).

Campaign DMC-DAF

This 1.5-hour-long campaign, running in 27 August 2016, comprised detailed monitoring of (i) CO_2 concentrations in EC during DAF ventilation mode before/after specific combination of door opening and (ii) the airflows through the individual cave doors after door opening. Data on CO_2 concentrations showed two periods with different CO_2 trends (Fig. 6). In the initial period (~30 minutes) under closed-door conditions, CO_2 concentrations slightly decreased from 1,176 to 799 ppmv, which corresponds to a removal of the anthropogenic CO_2 produced by last visitor group. After opening of the doors #2, #3, and CD, this concentrations rapidly increased during a relatively short period (~15 minutes) up to 2,500 ppmv. After

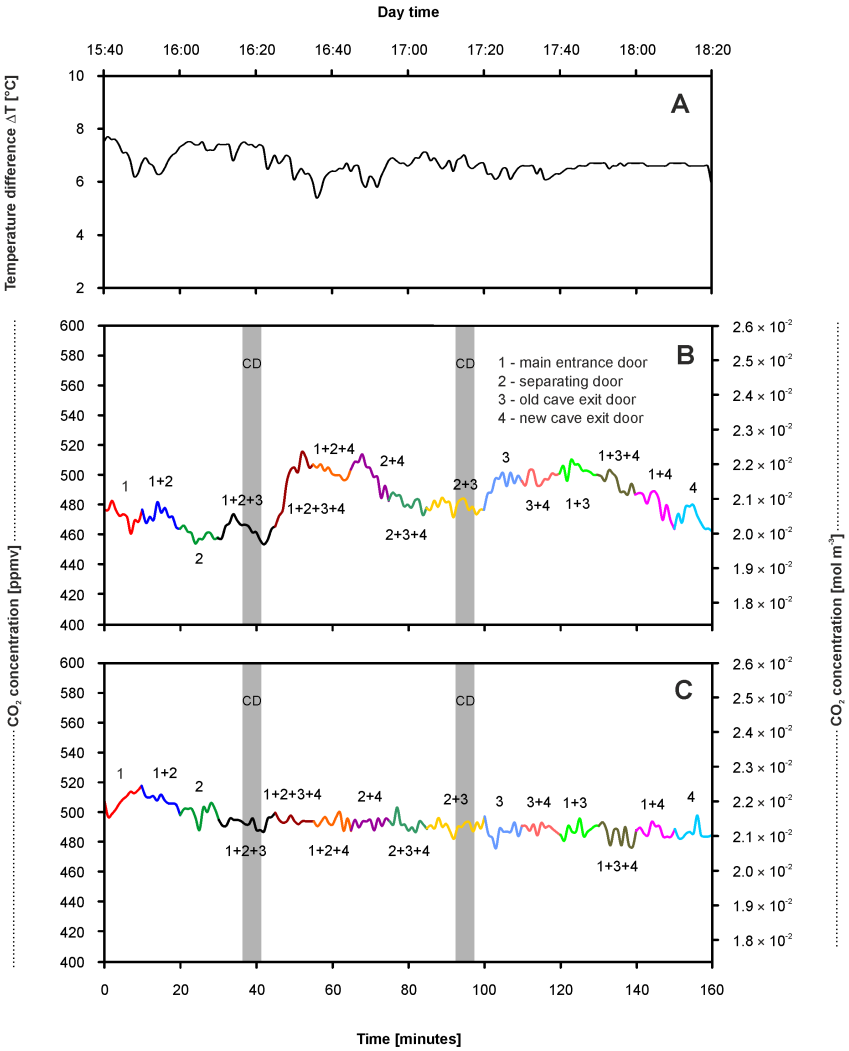

Fig. 4. Data from the campaign C3-DAF (29 April 2016; Balcarka Cave): temperature difference ΔT (A) and CO_2 concentrations in Entrance Chamber (B) and Gallery Chamber (C). The numbers at curves represent numbers of the doors open for given period. The grey bars represent the periods with opened connecting door CD. See text for details.

this, CO_2 concentrations only slightly increased up to 2,800 ppmv.

Independently from the CO_2 concentrations, the airflow directions/rates through the individual doors were logged except for the door #1 (main entrance) because of the poorly defined relative large vents around the door that did not allow for quantification. The results of airflow monitoring are summarized in Table 3. The monitored airflows through doors #2, #3, and #4 were out of EC and cave, respectively. The airflows through CD went into CC. The mean airflow rates showed a wide range of values for individual doors. Whereas the lower airflow rates up to 1.36×10^{-1} and 1.99×10^{-1} m^3 s^{-1} were found through the doors #3 (old cave exit door) and #2 (separating door), enhanced airflows reaching up to 3.83×10^{-1} m^3 s^{-1} were detected through the door #4 (new cave exit door).

DATA ANALYSIS

During UAF ventilation mode, the CO_2 concentrations in both chambers evolved predictably: the concentrations slightly decreased in EC and remained almost constant in GC (Fig. 2). During DAF mode, however, a completely different CO_2 behavior was observed, especially in EC: the door opening led to increase of CO_2 levels (Figs. 3, 4, and 5). Furthermore, different CO_2 levels in EC caused by opening of individual cave doors were identified. Opening of the separating door (#2) and old cave exit door (#3) were found to be responsible for observed increase of CO_2 levels. Moreover, this effect was amplified by opening CD. In contrast, opening of new cave exit door (#4) through all the combinations contributes to the decrease of CO_2 levels. Comparison of the airflow rates through the individual doors (Table 3) indicates that airflows through the door #4 roughly represent a sum of both partial airflows through the doors #2 and #3.

The total CO_2 flux responsible for the increase was calculated from detailed data (Fig. 6) based on Eqn. 5. Its value was j ~1.1×10^{-2} mol s^{-1}. For better understanding of the phenomenon, individual CO_2 fluxes potentially contributing to the total flux were estimated. The assumed fluxes were: (1) diffusive flux from soils/epikarst, (2) advective fluxes from deeper cave passages, and (3) direct advective flux from epikarst. The fluxes resulting from dripwater degassing were not included because of their assumed low values (see Lang et al., 2016) and constancy during the whole monitoring campaign.

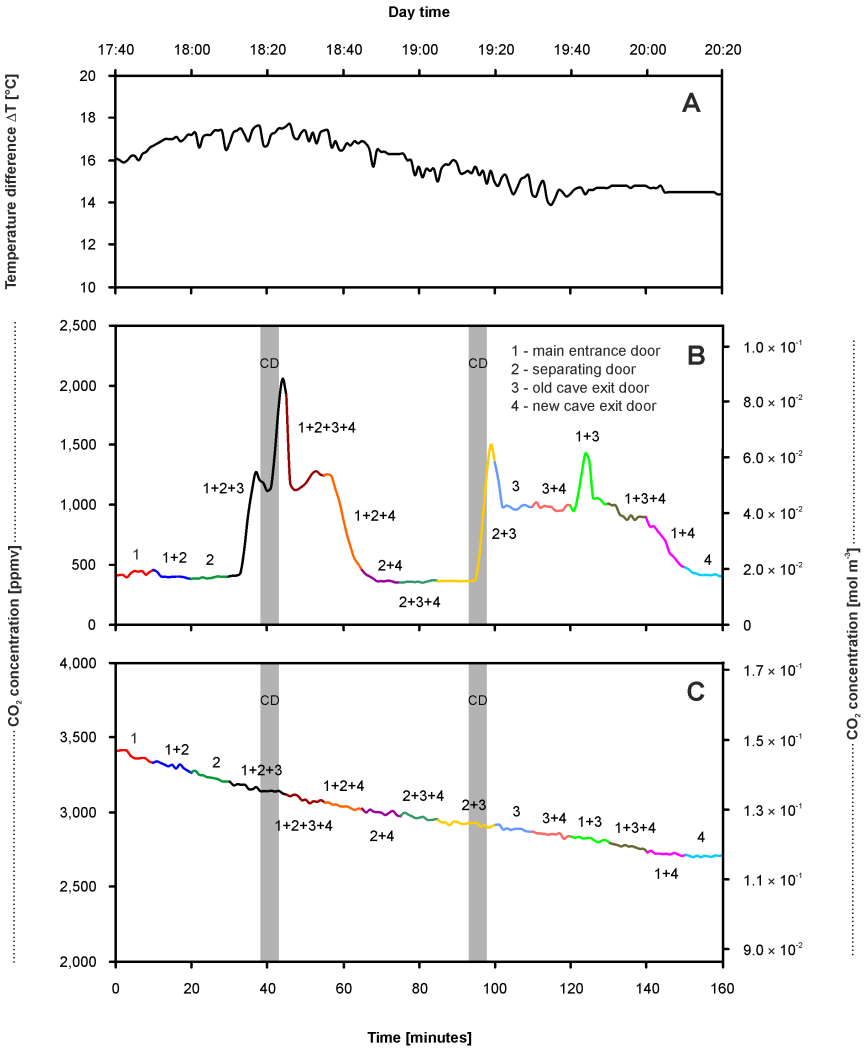

Fig. 5. Data from the campaign C4-DAF (30 July 2016; Balcarka Cave): temperature difference ΔT (A) and CO_2 concentrations in Entrance Chamber (B) and Gallery Chamber (C). The numbers at curves represent numbers of the doors open for given period. The grey bars represent the periods with opened connecting door CD. See text for details.

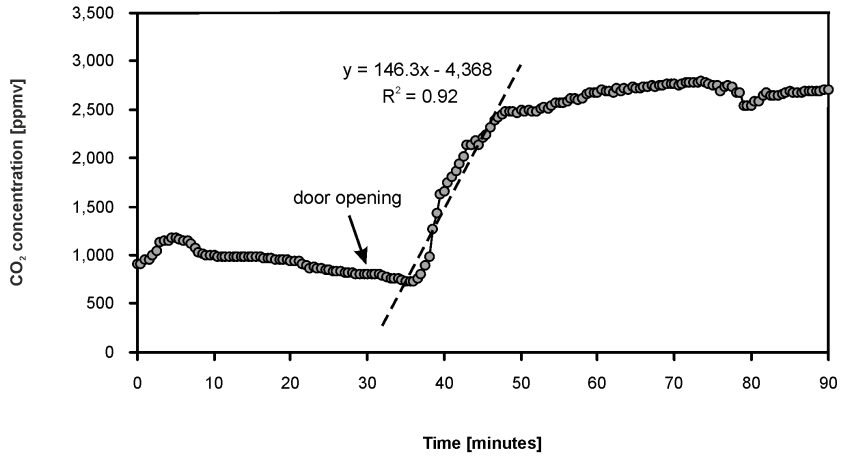

Fig. 6. Data from the campaign DMC-DAF (27 August 2016, Balcarka Cave): CO_2 concentrations in Entrance Chamber before/after opening the doors #2, #3, and CD. See text for details.

The input diffusive CO_2 flux from soils/epikarst into EC, j_{dif}^{EK} [mol s^{-1}], was estimated from Eqn. (2). Both extreme values of CO_2 diffusivity (1.0×10^{-7} and 1.4×10^{-5} m^2 s^{-1}) were applied, in order to cover nonhomogeneous structure of cave overburden. The CO_2 concentrations directly measured in upper parts of the soil profiles in the Moravian Karst range from 1,000 to 10,000 ppmv (4.3×10^{-2} to 0.43 mol m^{-3}) (Faimon & Ličbinská, 2010; Faimon et al., 2012b; Blecha & Faimon, 2014). A narrower range is reported for cave CO_2 concentrations. The Balcarka Cave belongs to the caves with rather low CO_2 levels, between 500 and 3,000 ppmv (2.2×10^{-2} and 2.0×10^{-1} mol m^{-3}) (Faimon et al., 2012b; Lang et al., 2016). According to the cave altitude diagram (Fig. 1B), the distance for diffusive CO_2 transport, ΔL, roughly corresponds to

Table 3. Airflow monitoring of the individual cave doors.

Door	Airflow direction	Volumetric airflow rate [$m^3 s^{-1}$]
#1	into the cave	n.m.
#2	out of the chamber	$(0.83\text{-}1.36) \times 10^{-1}$
#3	out of the cave	$(0.10\text{-}1.99) \times 10^{-1}$
#4	out of the cave	$(1.78\text{-}3.83) \times 10^{-1}$
CD	toward CC	n.m.

n.m. – not measured

40 m. Based on all the estimated ranges of individual variables and the total diffusion area of about 28 m^2 (the projected area of EC), the direct diffusive CO_2 flux into EC, j_{dif}^{EK}, should range between 1.5×10^{-9} and 3.9×10^{-6} mol s^{-1} (see Table 4).

The input advective CO_2 fluxes into EC, j_{adv} [mol s^{-1}], were estimated from Eqn. (3). Two types of such fluxes were distinguished: (i) the input advective flux from deeper cave passages (GC was used as the representative one), j_{adv}^{Gal}, and (ii) input advective flux from soils/epikarst, j_{adv}^{EK}. Both fluxes were driven by cave airflows, Q [m^3 s^{-1}], and the source CO_2 concentration [mol m^{-3}] (c_{Gal} for GC and c_{EK} for soils/epikarst). The volumetric airflow rates through the door #2 in the DAF mode varied in the range of $(0.83\text{-}1.36) \times 10^{-1}$ m^3 s^{-1} (Table 3). The CO_2 concentrations in GC during campaigns at DAF mode ranged between 476 and 3,413 ppmv (2.1×10^{-2} and 0.15 mol m^{-3}) (Figures 3C, 4C, and 5C). Based on the estimated ranges of individual variables, the advective CO_2 fluxes into EC from GC, j_{adv}^{Gal}, would range from 1.7×10^{-3} to 2.0×10^{-2} mol s^{-1} and from the soils/epikarst, j_{adv}^{EK}, from 3.6×10^{-3} to 5.9×10^{-2} mol s^{-1}. All the calculated advective fluxes are summarized in Table 4.

Distinction between the advective fluxes was deduced from estimated transport time. The calculation was based on the volumetric airflow rates measured at the door #2 of $(0.83\text{-}1.36) \times 10^{-1}$ m^3 s^{-1} (Table 3) and individual cross-section areas through which CO_2 is transported into EC. The cross-section area of the corridor connecting EC with GC is about 10 m^2 on average. Total cross-section area of the fissures, cracks, and shafts in EC overburden (the area for advective CO_2 fluxes from epikarst) was estimated to be less than 1 m^2. Based on these individual parameters, the estimated linear airflow rates for CO_2 transport from epikarst into EC were in the ranges of $(0.8\text{-}1.4) \times 10^{-2}$ m s^{-1} and $(4.2\text{-}6.8) \times 10^{-2}$ m s^{-1} into GC. Assuming the distance EC vs. GC of ~100 m and the thickness of EC overburden of ~50 m the transport time is from 2.0 to 3.3 hours from GC and up to 0.1 hours from epikarst.

Table 4. Overview of CO_2 fluxes into EC.

flux*	parameter					value	units
	D [m^2 s^{-1}]	Δc [mol m^{-3}]	ΔL [m]	c [mol m^{-3}]	Q [m^3 s^{-1}]		
j_{dif}^{EK}	1.0×10^{-7} to 1.4×10^{-5}	2.2×10^{-2} to 0.4	40	n.u.	n.u.	1.5×10^{-9} to 3.9×10^{-6}	[mol s^{-1}]
j_{adv}^{Gal}	n.u.	n.u.	n.u.	2.1×10^{-2} to 0.15	8.3×10^{-2} to 0.14	1.7×10^{-3} to 2.0×10^{-2}	[mol s^{-1}]
j_{adv}^{EK}	n.u.	n.u.	n.u.	4.3×10^{-2} to 0.43	8.3×10^{-2} to 0.14	3.6×10^{-3} to 5.9×10^{-2}	[mol s^{-1}]

*see List of Simbols; n.u. – not used

DISCUSSION

The CO_2 concentrations measured in the Balcarka Cave in the range from 300 to 3,500 ppmv roughly agree with the values previously measured in the Moravian Karst caves (Faimon et al., 2006; Faimon et al., 2012a; Lang et al., 2015a, b, 2016, 2017) and also with the values reported by, e.g., Spötl et al. (2005), Baldini et al. (2006), Liñán et al. (2008), Lario & Soler (2010), and Ridley et al. (2015). The range of values indicates that Balcarka Cave belongs to the caves significantly influenced by cave ventilation (e.g., Kowalczk & Froelich, 2010; Tremaine et al., 2011). Based on Lang et al. (2016), the Balcarka Cave represents the cave of geometry A, characterized by an open lower entrance and the upper hidden openings allowing the air/CO_2 to penetrate into the cave through soils/epikarst. Whereas the lower CO_2 levels are associated with the UAF ventilation mode, higher levels are associated with DAF mode (due to the direct advective CO_2 fluxes from soils/epikarst). A different CO_2 variability was identified in the individual chambers. Whereas the wide ranges of CO_2 levels are visible in the EC representing cave entrance passages, significantly narrower ranges were found in the GC situated in deeper cave passages (Fig. 1A). This is consistent with lower-variable CO_2 levels generally found in deeper cave passages (e.g., Buecher, 1999; Baldini et al., 2006). This also explains why the effect of door opening in GC was attenuated during the monitoring campaigns (Figs. 2-5).

Under the UAF mode, the opening of cave doors contributed to a general increase of cave airflows and advective output CO_2 fluxes, which led to decrease of CO_2 levels. This effect is evident in the cave entering passages (EC). Under DAF mode, the cave door opening caused a switching of predominant airflow paths that changed the main CO_2 sources and fluxes. This resulted in increase of the CO_2 levels in EC while the CO_2 levels in GC decreased. The mechanism of switching ventilation branches/paths is little understood and requires further study. However, it seems evident that in case of two parallel ventilation paths, the airflows would dominate in the paths with lower resistance (the resistance could be driven by the morphology/topography/segmentation and length of individual paths). The input flux increase in EC is well documented by CO_2 peaks in the campaigns C2-DAF and C4-DAF reaching the maxima up to 1,200 ppmv (5.2×10^{-2} mol m^{-3}) (Fig. 3B) and even 2,100 ppmv (9.1×10^{-2} mol m^{-3}) (Fig. 5B), respectively. Such rapid increase of the CO_2 in EC is caused by

strong input CO_2 fluxes. Because of downward airflows (DAF mode), the CO_2 sources of the fluxes should be situated in the upper cave parts: in (i) GC, (ii) CC or (iii) epikarst/soils. Analysis of potential input fluxes is given in Table 4. Direct diffusive CO_2 fluxes from overburden show too low values (between 1.5×10^{-9} and 3.9×10^{-6} mol s^{-1}) to cover the total flux into EC. In contrast, the advective CO_2 fluxes from the deeper cave passages (GC) show the values ranging from 1.7×10^{-3} to 2.0×10^{-2} mol s^{-1} that are comparable with the experimentally found total flux into EC (1.1×10^{-2} mol s^{-1}). However, the transport time of CO_2 would be too long (2.0 to 3.3 hours). It would result in several hours' lag, which is inconsistent with data. The airflow directions through doors #2 and #3 pointing out of the chamber/cave (Table 3) question the possibility of flux from the CC. Moreover, the transport time would be even longer than from the GC. At given airflows, strong CO_2 fluxes could result from the high CO_2 concentrations in soils/epikarst. Thus, the advective input fluxes from epikarst (3.6×10^{-3} to 5.9×10^{-2} mol s^{-1}) remain the more probable fluxes causing the increase of CO_2 levels in EC at the changes of ventilation during the DAF mode. The CO_2 transport time from epikarst reaching 0.1 hour is roughly consistent with the lag of CO_2 levels (~15 minutes) beyond the door opening (Fig. 6). There are even conceivable sudden changes of cave CO_2 levels by the advective fluxes from epikarst without lag, made by a "piston flow" (see, e.g., Baldini et al., 2008).

The lower CO_2 levels (about 480 ppmv, i.e., 2.1×10^{-2} mol m^{-3} on average) with fluctuations found during the campaign C3-DAF (Fig. 4B) could be explained by transitionally lower CO_2 concentrations in soils/epikarst. The campaign C3-DAF was conducted in April, when CO_2 concentrations in soils did not reach the "standard" summer values and cave CO_2 levels corresponded to winter levels. Some studies on CO_2 concentrations in the soils above the Balcarka Cave (e.g., Faimon et al., 2012b) showed roughly half-values during spring (April to May) in comparison with summer season (June to August). The campaigns C2-DAF and C4-DAF were performed in July, when maxima of CO_2 concentrations in soils are generally reached. In fact, this explanation seems to be somehow contradicting to the previous studies of Faimon et al. (2012c) and Pracný et al. (2016a, b) indicating only slight seasonal variations in epikarstic CO_2 concentrations. Thus, this seasonality in CO_2 fluxes may indicate that soils are the main source of CO_2 in the Balcarka Cave. An additional reason for the inconsistencies in CO_2 levels could be the lower ΔT values corresponding to weaker airflows at the campaign C3-DAF (Faimon & Lang, 2013).

An analysis of the experimentally found airflow directions and the altitude relations of cave geometry allowed to estimate possible ventilation paths throughout the Balcarka Cave at open doors (#2, #3, #4 and CD) for individual ventilation modes (Fig. 7). Detailed patterns of airflows in the cave with closed door are not known. It would require a special study with specific monitoring equipment, which was not in the scope of this article. In fact, despite the closed doors, the cave ventilates and shows the seasonality typical for dynamic caves. No doubt, various hidden/unknown openings play a role. However, the regime of ventilation changes at open doors.

Scheme of the airflow paths during UAF mode showed three main branches of the airflow from exterior: (i) one branch through the doors #1 and CD, (ii) second branch through the door #2, EC and GC, and (iii) third branch through the doors #3 and #4 (Fig. 7A). All the airflows reoriented towards the CC and back to exterior by the chimney. The doors #1 and #3 are playing the role of both lower and upper entrances concurrently. Measurement at these doors indicates that the cold air may flow through the door at the ground whereas the warmer air at the top. The monitored chambers EC and GC are vented by the

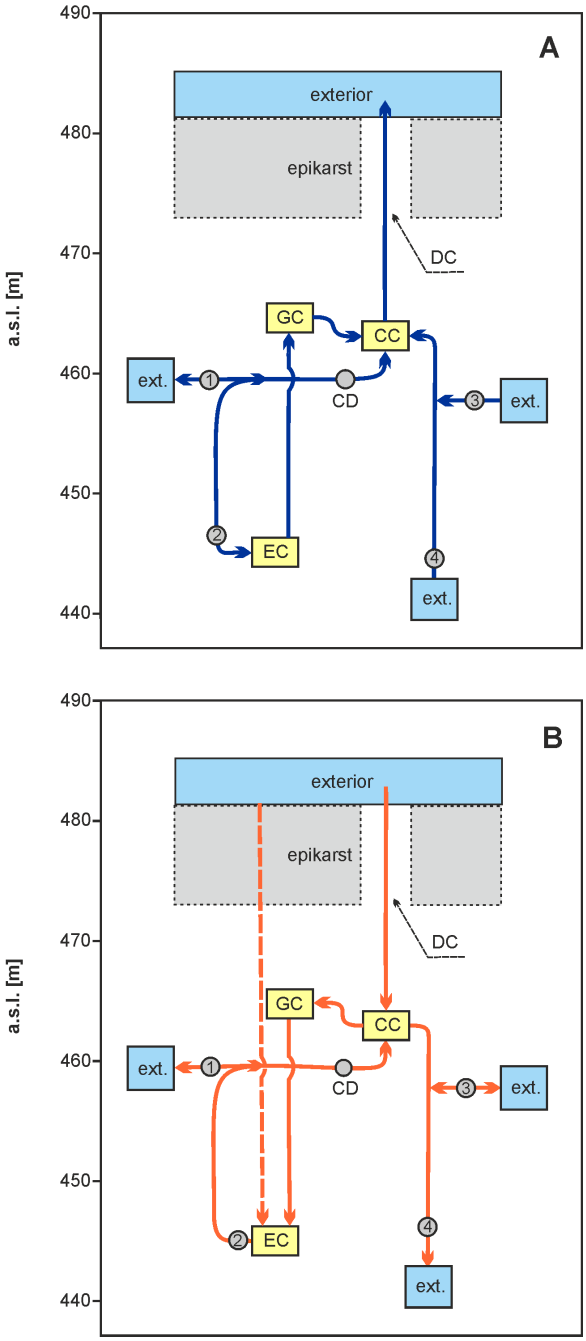

Fig. 7. The altitude diagram of the individual cave passages with marked ventilation paths under UAF (A) and DAF (B) ventilation mode. The acronym DC corresponds to the Discovers' Chimney. The horizontal axis is not in scale.

second ventilation branch. The gradual decrease of CO_2 levels in EC resulted from the direct transport of low CO_2 concentrations from exterior and cave entrance passages (Fig. 2B, C). In the remote cave parts (GC), the instantaneous change in CO_2 cannot be observed during such short-term ventilation change.

During the DAF mode, the ventilation paths completely changed (Fig. 7B). Additional airflows through the epikarst bringing significant amount of CO_2 are probably responsible for the higher CO_2 concentrations in EC (Figs. 3B and 5B). It could be demonstrated by instantaneous changes in CO_2 isotopic composition, but relevant data were not available. We will concentrate on this issue in a future study. The gradual decrease of CO_2 levels in GC (Figs. 3C and 5C) could be associated with the enhanced airflow between CC – GC – EC (through the doors #2). The long distance between EC and GC did not allow the impact on the CO_2 levels in EC. The airflow rates through the door #4 (Table 3) confirm summarization of the partial airflows through doors #2 and #3.

The study showed that just one additional entrance could be crucial at the setting of ventilation regime in a cave. This important finding should be remembered during discovering and accessing of caves. In the case of the Balcarka Cave, the lowest entrance (the door #4) is responsible for the main reduction in cave CO_2 levels. The combinations of open separating doors #2, old cave entrance #3, and connecting doors CD are responsible for increase in the cave CO_2 levels (especially in EC during DAF mode). Since neither door #3 nor CD are commonly used, no revision of the current visitors' regime in the Balcarka Cave is necessary. Generally, however, the effect of simultaneously open door needs to be assessed on a case-by-case basis.

CONCLUSIONS

The impact of door opening on cave CO_2 concentrations was studied in (i) the Entrance Chamber and (ii) the Gallery Chamber of the Balcarka Cave (Moravian Karst). The results showed that CO_2 levels in both the studied cave sites were influenced by different factors depending on the external and internal conditions. Based on the opening of individual doors, different ventilation paths were distinguished in the cave under upward airflow (UAF) and downward airflow (DAF) ventilation modes. During the UAF mode, the cave door opening contributed to general increase of cave airflows and thus to the decrease of CO_2 concentrations due to enhanced output advective CO_2 fluxes. Such effect was evident especially in the Entrance Chamber due to the transport of lower CO_2 concentrations from cave entrance passages. In the Gallery Chamber situated deeper in the cave, such effect was suppressed. During the DAF mode, some combinations of door opening lead to the changes in cave airflow paths. With the change, also main CO_2 sources changed, which paradoxically lead to significant CO_2 level increase in the Entrance Chamber. Modeling suggested that just the transport of enhanced CO_2 concentrations from epikarst by advective fluxes represents the more probable factor causing the increase. The study has shown that even short-term changes in cave ventilation may radically influence cave microclimate. Therefore, some organizational and technical measures are proposed in the more frequent show caves, in order to keep natural conditions. They could be associated with automatic door closers or/and with a harmonization of the entry/exit times of individual visitor groups in order to prevent the opening of several doors simultaneously. This study focused on the show caves could also contribute to the general knowledge about possible changes in cave microclimate in the geological past, during which old openings were periodically closed by sediments at various events (collapses, floods) while new openings were created.

ACKNOWLEDGEMENTS

The authors thank three anonymous reviewers for their valuable comments that contribute to improving this article. Furthermore, the authors thank colleagues Ondra Sracek and Pavel Pracný for critically reading the manuscript. The Cave Administration of Czech Republic is thanked for wide support. The research was supported by the funding from Masaryk University (Brno) and Palacký University (Olomouc).

REFERENCES

Baker A. & Genty D., 1998 - *Environmental pressures on conserving cave speleothems: effects of changing surface land use and increased cave tourism.* Journal of Environmental Management, **53 (2)**: 165-175. https://doi.org/10.1006/jema.1998.0208

Baldini J.U.L., Baldini L.M., McDermott F. & Clipson N., 2006 - *Carbon dioxide sources, sinks, and spatial variability in shallow temperate zone caves: Evidence from Ballynamintra Cave, Ireland.* Journal of Cave and Karst Studies, **68 (1)**: 4-11.

Baldini J.U.L., McDermott F., Hoffmann D.L., Richards D.A. & Clipson N., 2008 - *Very high-frequency and seasonal cave atmosphere PCO_2 variability: Implications for stalagmite growth and oxygen isotope-based paleoclimate records.* Earth and Planetary Science Letters, **272**: 118-129. https://doi.org/10.1016/j.epsl.2008.04.031

Banner J.L., Guilfoyle A., James E.W. Stern L.A & Musgrove M., 2007 - *Seasonal variations in modern speleothem calcite growth in Central Texas, USA.* Journal of Sedimentary Research, **77**: 615-622. https://doi.org/10.2110/jsr.2007.065

Blecha M. & Faimon J., 2014 - *Spatial and temporal variations in carbon dioxide (CO2) concentrations in selected soils of the Moravian Karst (Czech Republic).* Carbonates and Evaporites, **29 (4)**: 395-408. https://doi.org/10.1007/s13146-014-0220-7

Bourges F., Mangin A. & d'Hulst, D., 2001 - *Carbon dioxide in karst cavity atmosphere dynamics: the example of the Aven d'Orgnac (Ardéche).* Earth and Planetary Sciences, **333 (11)**: 685-692. https://doi.org/10.1016/S1251-8050(01)01682-2

Buecher R.H., 1999 - *Microclimate study of Kartchner Caverns, Arizona.* Journal of Cave and Karst Studies, **61 (2)**: 108–120.

Calaforra J.M., Fernández-Cortés A., Sánchez-Martos F., Gisbert J. & Pulido-Bosch A., 2003 - *Environmental control for determining human impact and permanent visitor capacity in a potential sow cave before tourist use.* Environmental Conservation, **30 (2)**: 160-167. https://doi.org/10.1017/S0376892903000146

Cigna A.A., 1968 - *An analytical study of air circulation in caves.* International Journal of Speleology, **3**: 41-54. https://doi.org/10.5038/1827-806X.3.1.3

Davidson E.A. & Trumbore S.E., 1995 - *Gas diffusivity and production of CO_2 in deep soils of the eastern Amazon.* Tellus, Series B – Chemical and Physical Meteorology, **47 (5)**: 550-565. https://doi.org/10.3402/tellusb.v47i5.16071

de Freitas C.R., Littlejohn R.N., Clarkson T.S. & Kristament I.S., 1982 - *Cave climate: assessment of airflow and ventilation.* Journal of Climatology, **2**: 383-397. https://doi.org/10.1002/joc.3370020408

de Freitas C.R. & Schmekal, A., 2006 - *Studies of condensation/evaporation processes in the Glowworm Cave, New Zealand.* International Journal of Speleology, **35 (2)**: 75-81. https://doi.org/10.5038/1827-806X.35.2.3

de Freitas C.R., 2010 - *The role and importance of cave microclimate in the sustainable use and management of show caves.* Acta Carsologica, **39 (3)**: 477-489. https://doi.org/10.3986/ac.v39i3.77

Dreybrodt W., 1999 - *Chemical kinetics, speleothem growth and climate.* Boreas, **28**: 347-356. https://doi.org/10.1080/030094899422073

Dublyansky V.N. & Dublyansky Y.V., 1998 - *The problem of condensation in karst studies.* Journal of Cave and Karst Studies, **60 (1)**: 3-17.

Faimon J., Štelcl J. & Sas D., 2006 - *Anthropogenic CO_2-flux into cave atmosphere and its environmental impact: A case study in the Císařská Cave (Moravian Karst, Czech Republic).* Science of the Total Environment, **369**: 231-245. https://doi.org/10.1016/j.scitotenv.2006.04.006

Faimon J. & Ličbinská M., 2010 - *Carbon dioxide in the soils and adjacent caves of the Moravian Karst.* Acta Carsologica, **39 (3)**: 463-475. https://doi.org/10.3986/ac.v39i3.76

Faimon J., Troppová D., Baldík V. & Novotný R., 2012a - *Air circulation and its impact on microclimatic variables in the Císařská Cave (Moravian Karst, Czech Republic).* International Journal of Climatology, **32**: 599-623. https://doi.org/10.1002/joc.2298

Faimon J., Ličbinská M. & Zajíček P., 2012b - *Relationship between carbon dioxide in Balcarka Cave and adjacent soils in the Moravian Karst region of the Czech Republic.* International Journal of Speleology, **41 (1)**: 17-28. https://doi.org/10.5038/1827-806X.41.1.3

Faimon J., Ličbinská M., Zajíček P. & Sracek O., 2012c - *Partial pressures of CO_2 in epikarstic zone deduced from hydrogeochemistry of permanent drips, the Moravian Karst, Czech Republic.* Acta Carsologica, **41 (1)**: 47-57. https://doi.org/10.3986/ac.v41i1.47

Faimon J. & Lang M., 2013 - *Variances in airflows during different ventilation modes in a dynamic U-shaped cave.* International Journal of Speleology, **42 (2)**: 115-122. https://doi.org/10.5038/1827-806X.42.2.3

Fairchild I.J., Borsato A., Tooth A.F., Frisia S., Hawkesworth C.J., Huang Y., McDermott F. & Spiro B., 2000 - *Controls on trace element (Sr-Mg) compositions of carbonate cave waters: implications for speleothem climatic records.* Chemical Geology, **166**: 255-269. https://doi.org/10.1016/S0009-2541(99)00216-8

Fernández P.L., Gutierrez I., Quindós L.S. Soto J. & Villar E., 1986 - *Natural ventilation of the Paintings Room in the Altamira cave.* Nature, **321**: 586-588. https://doi.org/10.1038/321586a0

Ford T.D. & Williams P.W., 2007 - *Karst hydrogeology and geomorphology.* Wiley & Sons, Chicester, 576 p.

Frisia S., Fairchild I.J., Fohlmeister J., Miorandi R., Spötl C. & Borsato A., 2011 - *Carbon massbalance modeling and carbon isotope exchange processes in dynamic caves.* Geochimica et Cosmochimica Acta, **75**: 380-400. https://doi.org/10.1016/j.gca.2010.10.021

Holland H.D., Kirsipu T.V., Huebner J.S. & Oxburgh U.M., 1964 - *On some aspects of the chemical evolution of cave water.* Journal of Geology, **72**: 36-67. https://doi.org/10.1086/626964

Hoyos M., Soler V., Cañaveras J.C., Sánchez-Moral S. & Sanz-Rubio E., 1998 - *Microclimatic characterization of a karstic cave: human impact on microenvironmental parameters of a prehistoric rock art cave (Candamo Cave, northern Spain).* Environmental Geology, **33 (4)**: 231-242. https://doi.org/10.1007/s002540050242

Kowalczk A.J. & Froelich P.N., 2010 - *Cave air ventilation and CO_2 outgassing by radon-222 modeling: How fast do caves breath?* Earth and Planetary Science Letters, **289**: 209-219. https://doi.org/10.1016/j.epsl.2009.11.010

Lang M., Faimon J. & Ek C., 2015a - *The relationship between carbon dioxide concentration and visitor numbers in the homothermic zone of the Balcarka Cave (Moravian Karst) during a period of limited ventilation.* International Journal of Speleology, **44 (2)**: 167-176. https://doi.org/10.5038/1827-806X.44.2.6

Lang M., Faimon J. & Ek C., 2015b - *A case study of anthropogenic impact on the CO_2 levels in low-volume profile of the Balcarka Cave (Moravian Karst, Czech Republic).* Acta Carsologica, **44 (1)**: 71-80. https://doi.org/10.3986/ac.v44i1.917

Lang M., Faimon J., Godissart J. & Ek, C., 2016 - *Carbon dioxide seasonality in dynamically ventilated caves: the role of advective fluxes.* Theoretical and Applied Climatology, (in print). https://doi.org/10.1007/s00704-016-1858-y

Lang M., Faimon J., Pracný P. & Kejíková S., 2017 - *A show cave management: Anthropogenic CO_2 in atmosphere of Výpustek Cave (Moravian Karst, Czech Republic).* Journal for Nature Conservation, **35**: 40-52. https://doi.org/10.1016/j.jnc.2016.11.007

Lario J. & Soler V., 2010 - *Microclimate monitoring of Pozalagua Cave (Vizcaya, Spain): application to management and protection of show caves.* Journal of Cave and Karst Studies, **72 (3)**: 169-180. https://doi.org/10.4311/jcks2009lsc0093

Lasaga A.C. & Berner R.A., 1998 - *Fundamental aspects of quantitative models for geochemical cycles.* Chemical Geology, **145**: 161-175. https://doi.org/10.1016/S0009-2541(97)00142-3

Liñán C., Vadillo I. & Carrasco F., 2008 - *Carbon dioxide concentration in air within the Nerja Cave (Malaga, Andalusia, Spain).* International Journal of Speleology, **37**: 99-106. https://doi.org/10.5038/1827-806X.37.2.2

Lobo H.A.S., 2015 - *Tourist carrying capacity of Santana cave (PETAR-SP, Brazil): A new method based on a critical atmospheric parameter.* Tourism Management Perspectives, **16**: 67-75. https://doi.org/10.1016/j.tmp.2015.07.001

Luetscher M. & Jeannin P.-Y., 2004 - *Temperature distribution in karst systems: the role of air and water fluxes.* Terra Nova, **16**: 344-350. https://doi.org/10.1111/j.1365-3121.2004.00572.x

Milanolo S. & Gabrovšek F., 2009 - *Analysis of Carbon Dioxide Variations in the Atmosphere of Srednja Bijambarska Cave, Bosnia and Herzegovina.* Boundary-Layer Meteorology, **131**: 479-493. https://doi.org/10.1007/s10546-009-9375-5

Milanolo S. & Gabrovšek F., 2015 - *Estimation of carbon dioxide flux degassing from percolating waters in a karst cave: Case study from Bijambare cave, Bosnia and Herzegovina.* Chemie Der Erde-Geochemistry, **75**: 465-474. https://doi.org/10.1016/j.chemer.2015.10.004

Peyraube N., Lastennet R., Denis A. & Malaurent, P., 2013 - *Estimation of epikarst air P_{CO2} using measurements of water $\delta^{13}C_{TDIC}$, cave air P_{CO2} and $\delta^{13}C_{CO2}$.* Geochimica et Cosmochimica Acta, **118**: 1-17. https://doi.org/10.1016/j.gca.2013.03.046

Pracný P., Faimon J., Kabelka L. & Hebelka J., 2016a - *Variations of carbon dioxide in the air and dripwaters of Punkva Caves (Moravian Karst, Czech Republic).* Carbonates and Evaporites, **31 (4)**: 375-386. https://doi.org/10.1007/s13146-015-0259-0

Pracný P., Faimon J., Sracek O., Kabelka L., Hebelka J., 2016b - *Anomalous drip in the Punkva caves (Moravian Karst): relevant implications for paleoclimatic proxies.* Hydrological Processes, **30 (10**): 1506-1520. https://doi.org/10.1002/hyp.10731

Pulido-Bosch A., Martín-Rosales W., López-Chicano M., Rodríguez-Navarro C.M. & Vallejos A., 1997 - *Human impact in a tourist karstic cave (Aracena, Spain).* Environmental Geology, **31 (3/4)**: 142-149. https://doi.org/10.1007/s002540050173

Richon P., Perrier F., Sabroux J.-C., Trique M., Ferry C., Voisin V. & Pili E., 2005 - *Spatial and time variations of radon-222 concentration in the atmosphere of a dead-end horizontal tunel.* Journal of Environmental Radioactivity, **78**: 179–198. https://doi.org/10.1016/j.jenvrad.2004.05.001

Ridley H.E., Baldini J.U.L., Prufer K.M., Walczak I.W. & Breitenbach S.F.M., 2015 - *High-resolution monitoring of Yok Balum Cave, Belize: An investigation of seasonal ventilation regimes and the atmospheric and drip-flow response to a local earthquake.* Journal of Cave and Karst Studies, **77 (3)**: 183-199. https://doi.org/10.4311/2014ES0117

Sánchez-Moral S., Soler V., Cañaveras J.C., Sanz-Rubio E., Van Grieken R. & Gysels K., 1999 - *Inorganic deterioration affecting the Altamira Cave, N Spain: quantitative approach to wall-corrosion (solutional etching) processes induced by visitors.* Science of the Total Environment, **243/244**: 67-84. https://doi.org/10.1016/S0048-9697(99)00348-4

Sarbu S.M. & Lascu C., 1997 - *Condensation corrosion in Movile cave, Romania.* Journal of Cave and Karst Studies, **59**: 99-102.

Schlesinger W.H. & Andrews J.A., 2000 - *Soil respiration and the global carbon cycle.* Biogeochemistry, **48**: 7-20. https://doi.org/10.1023/A:1006247623877

Šebela S., Prelovšek M. & Turk J., 2013 - *Impact of peak period visits on the Postojna Cave (Slovenia) microclimate.* Theoretical and Applied Climatology, **111 (1-2)**: 51-64. https://doi.org/10.1007/s00704-012-0644-8

Šebela S. & Turk J., 2014 - *Natural and anthropgenic influences on the year-round temperature dynamics of air and water in Postojna show cave, Slovenia.* Tourism Management, **40**: 233-243. https://doi.org/10.1016/j.tourman.2013.06.011

Spötl C., Fairchild I.J. & Tooth, A.F., 2005 - *Cave air control on dripwater geochemistry, Obir Caves (Austria): implications for speleothem deposition in dynamically ventilated caves.* Geochimica et Cosmochimica Acta, **69 (10)**: 2451-2468. https://doi.org/10.1016/j.gca.2004.12.009

Stumm W. & Morgan J.J., 1996 - *Aquatic chemistry: chemical equilibria and rates in natural waters, 3rd Edition.* Wiley-Interscience, New York, 1040 p.

Tarhule-Lips R.F.A. & Ford D.C., 1998 - *Condensation corrosion in Caves on Cayman Brac and Isla de Mona.* Journal of Cave and Karst Studies, **60**: 84-95.

Tremaine D.M., Froelich P.N. & Wang Y., 2011 - *Speleothem calcite farmed in situ: modern calibration of $d^{18}O$ and $d^{13}C$ paleoclimate proxies in a continuously-monitored natural cave system.* Geochimica et Cosmochimica Acta, **75**: 4929-4950. https://doi.org/10.1016/j.gca.2011.06.005

Welty J.R., Wicks C.E., Wilson R.E. & Rorrer G.L., 2008 - *Fundamentals of Momentum, Heat, and Mass Transfer, 5th Edition.* Wiley, New York, 740 p.

White W.B., 1988 - *Geomorphology and hydrology of karst terrains.* Oxford University Press, New York, 464 p.

Wigley T.M.L. & Brown M.C., 1971 - *Geophysical applications of heat and mass transfer in turbulent pipe flow.* Boundary-Layer Meteorology, **1**: 300-320. https://doi.org/10.1007/BF02186034